Pakistan Veterinary Journal

ISSN: 0253-8318 (PRINT), 2074-7764 (ONLINE)
DOI: 10.29261/pakvetj/2026.143

RESEARCH ARTICLE

Position and Airway Pressure Dependent Right and Left Ventricular Flow with 3.0T Cardiac MRI in Dogs

Chang-eun Lee[1], Kichang Lee[1] and Hakyoung Yoon[1*]

[1]Department of Veterinary Medical Imaging, College of Veterinary Medicine, Jeonbuk National University, Iksan-si, Republic of Korea
*Corresponding author: knighttt7240@gmail.com

ARTICLE HISTORY (26-162)

Received: February 22, 2026
Revised: May 12, 2026
Accepted: May 15, 2026
Published online: June 15, 2026

Key words:
Canine heart
Cardiac index
Cardiovascular magnetic resonance (CMR)
Phase-contrast MRI (PC-MRI)
Positive airway pressure
Recumbency

ABSTRACT

High-field phase-contrast magnetic resonance imaging (PC-MRI) enables quantification of ventricular output, although measurements may be affected by anesthesia-related variables. The present study investigated the influence of recumbency and airway pressure on cardiac index derived from 3.0T two-dimensional PC-MRI in dogs. Six clinically asymptomatic client-owned dogs underwent PC-MRI at the aortic valve (AV) and pulmonic valve (PV). Imaging was performed under zero end-expiratory pressure (ZEEP) in three positions: supine (dorsal recumbency; DR), right lateral recumbency (RLR), and left lateral recumbency (LLR). The DR acquisition was repeated during a CPAP 10 condition, defined as sustained airway pressure of 10cmH_2O during brief apnea for PC-MRI acquisition. Left ventricular cardiac index (LV CI), right ventricular cardiac index (RV CI), and the RV/LV CI ratio were compared across these conditions. Differences were assessed using repeated-measures and paired analyses, and complementary estimation metrics were reported; nominal $P<0.05$ was considered significant. Under ZEEP, RV CI in both lateral recumbencies was approximately 14–15% higher than in DR, whereas LV CI showed smaller directional increases. In DR, LV CI and RV CI showed non-significant directional decreases of approximately 7–10% under CPAP 10 compared with ZEEP. These preliminary findings suggest that recumbency and airway-pressure conditions may contribute to measurable within-dog variation in PC-MRI–derived ventricular cardiac indices in anesthetized dogs, supporting the need for standardized acquisition conditions in future studies.

To Cite This Article: Lee C, Lee K and Yoon H, 2026. Position and airway pressure dependent right and left ventricular flow with 3.0t cardiac mri in dogs. Pak Vet J, 46(6): 1516-1524. http://dx.doi.org/10.29261/pakvetj/2026.143

INTRODUCTION

Phase-contrast magnetic resonance imaging (PC-MRI) provides noninvasive quantification of blood flow using velocity-encoded phase information (Nayak *et al.*, 2015). In human practice, it is routinely used for valve-related flow quantification, shunt assessment, and great-vessel flow evaluation across the cardiac cycle (Fratz *et al.*, 2013; Nayak *et al.*, 2015; Adriaans *et al.*, 2020). In contrast, veterinary cardiac MRI is typically performed under general anesthesia with mechanical ventilation, which can influence the cardiorespiratory state during acquisition (Hopper and Powell, 2013; Fries, 2024). Therefore, PC-MRI–derived flow metrics in dogs may be sensitive to acquisition conditions that are often treated as routine background settings (Drees *et al.*, 2015).

In small-animal cardiology, transthoracic echocardiography remains the principal imaging modality for routine assessment of cardiac structure and function because of its accessibility and repeatability (Hillis and Bloomfield, 2005; Keene *et al.*, 2019). However, echocardiographic assessment can be limited by acoustic windows and operator dependence (Gilbert *et al.*, 2010). For this reason, cardiovascular magnetic resonance (CMR) is increasingly adopted in referral centers to support quantitative cardiovascular assessment in dogs (Fries, 2024). Although standardized CMR protocols have been established in human practice, veterinary CMR requires species-specific acquisition and analysis strategies because of differences in heart size, heart rate, respiration, and routine anesthesia (Gilbert *et al.*, 2010; Kramer *et al.*, 2020; Fries, 2024). Foundational data that clarify sources of variability are therefore needed for

reproducible quantitative CMR applications in dogs (Gilbert *et al.*, 2010).

General anesthesia and mechanical ventilation can alter hemodynamics, including heart rate, arterial pressure, pulmonary mechanics, and venous return (Hopper and Powell, 2013; Fries, 2024; Bailey *et al.*, 2025). In addition, dogs are commonly positioned in dorsal, right lateral, or left lateral recumbency during imaging and anesthesia, and experimental studies in anesthetized, mechanically ventilated dogs have reported posture-related cardiopulmonary differences (Bornscheuer *et al.*, 1996; Gärtner *et al.*, 1996; García-Sanz *et al.*, 2020). Dorsal or supine positioning has been associated with higher heart rate, but lower arterial pressure, systemic vascular resistance, and biventricular stroke work compared with lateral positions (Bornscheuer *et al.*, 1996; Gärtner *et al.*, 1996). Airway pressure may further modify global hemodynamics under anesthesia. Positive end-expiratory pressure or continuous positive airway pressure (CPAP) has been linked to changes in functional residual capacity, cardiac output, and respiratory variations in arterial pressure (Riquelme *et al.*, 2005, Soares *et al.*, 2021; Ambrósio *et al.*, 2022; Sanchez *et al.*, 2024). Collectively, these findings suggest that recumbency and airway pressure may act as physiologic modifiers of hemodynamics during PC-MRI acquisition.

Despite this background, posture- and airway pressure–related variation in canine PC-MRI flow metrics at 3.0T has not been systematically characterized. Accordingly, this study used 3.0T PC-MRI to evaluate within-dog differences in left ventricular cardiac index and right ventricular cardiac index derived from valve-level forward flow, along with the RV/LV cardiac index ratio, across dorsal, right lateral, and left lateral recumbency. Measurements were obtained under zero end-expiratory pressure (ZEEP) and under the CPAP 10 condition. It was hypothesized that lateral recumbency would be associated with higher LV and RV cardiac indices than DR, whereas CPAP 10 would be associated with lower LV and RV cardiac indices than ZEEP in DR. The RV/LV cardiac index ratio was evaluated to determine whether proportional relationships between PV-derived and AV-derived forward-flow indices changed across conditions.

MATERIALS AND METHODS

Study design and animals: This prospective study was conducted at Jeonbuk National University in client-owned, clinically asymptomatic dogs not receiving cardiac medication. Owner consent was obtained, and the protocol was approved by the Institutional Animal Care and Use Committee (IACUC No. JBNU NON2025-059). No formal a priori sample size calculation was performed because published canine 3.0T PC-MRI data on recumbency- and airway-pressure-related changes in ventricular flow indices were not available to provide a reliable effect-size estimate. The sample size was therefore based on the availability of eligible client-owned dogs that could complete all repeated PC-MRI acquisitions under the same anesthetic session. The study was designed as an exploratory within-dog analysis, and the results were interpreted as preliminary estimates rather than definitive reference values.

Dogs were required to have no cardiovascular clinical signs. Mild mitral regurgitation (MR) was permitted only without echocardiographic evidence of cardiac remodeling; such dogs were classified as myxomatous mitral valve disease (MMVD) stage B1 according to the American College of Veterinary Internal Medicine consensus guidelines (Keene *et al.*, 2019). Mild tricuspid regurgitation (TR) was permitted only without echocardiographic evidence of pulmonary hypertension (peak TR velocity<3.0m/s). Dogs with moderate-to-severe regurgitation or pulmonary hypertension were excluded. Detailed echocardiographic screening findings, including MR/TR status, peak TR velocity, and MMVD stage where applicable, are summarized in Table 1. This cohort was not intended to represent a normal reference population; rather, it consisted of clinically asymptomatic client-owned dogs that met predefined cardiovascular screening criteria for repeated PC-MRI acquisition.

Anesthesia and physiologic control: Premedication consisted of butorphanol (0.2mg/kg IV). Anesthesia was induced with propofol (4–6mg/kg IV to effect), followed by endotracheal intubation and maintenance with isoflurane (1.0–1.5%) in 100% O_2 with controlled mechanical ventilation. Between PC-MRI acquisitions, ventilation was delivered using pressure-controlled ventilation. Inspiratory pressure was initially set at approximately 10cmH_2O and adjusted within approximately 10–15cmH_2O as needed, with a respiratory rate initially set at 12breaths/min, to maintain end-tidal CO_2 ($EtCO_2$) at approximately 35–45mmHg. Normal saline was administered intravenously at 5mL/kg/h during anesthesia. Electrocardiography, noninvasive blood pressure, and $EtCO_2$ were monitored continuously. This anesthetic protocol was selected as a standardized clinically applicable protocol for canine CMR because it allowed controlled ventilation, ECG gating, and continuous physiologic monitoring; it was not assumed to be free of cardiovascular or respiratory effects. To reduce protocol-related variability, all dogs were managed using the same anesthetic and ventilation framework, and data were acquired only during predefined physiologic stability periods (Hopper and Powell, 2013; Drees *et al.*, 2015; Bailey *et al.*, 2025).

Data were acquired only during stable periods, defined as heart rate (HR) and mean arterial pressure (MAP) within approximately ±10% of each dog's session mean. Immediately before each PC-MRI acquisition, ventilation was paused, and apnea was maintained for approximately 10–15s during image acquisition. Physical repositioning between recumbency conditions was generally completed within approximately 1min; before each subsequent acquisition, coil position, ECG gating, and physiologic stability were rechecked.

MRI system, protocol, and PC-MRI acquisition: Imaging was performed on a 3.0T system (uMR 780, United Imaging Healthcare, Shanghai, China) using uExceed software (Release R002) with a 32-channel spine coil and a 12-channel flexible surface coil secured over the thorax across recumbency conditions. Dogs were positioned head-first, and electrocardiographic (ECG) gating and heart-focused manual shimming were applied.

Flow acquisitions were performed in a fixed order: supine (dorsal recumbency; DR) under zero end-expiratory pressure (ZEEP), DR under CPAP 10, right lateral recumbency (RLR) under ZEEP, and left lateral recumbency (LLR) under ZEEP. Thus, both RLR and LLR were evaluated under ZEEP, whereas CPAP 10 was evaluated only in DR. In this study, CPAP 10 was used as an operational label for a sustained airway pressure of 10cmH_2O maintained during the brief apnea used for PC-MRI acquisition; it did not refer to spontaneous-breathing CPAP mode. During ZEEP acquisitions, no positive airway pressure was applied during the brief apnea. Immediately before each PC-MRI acquisition, mechanical ventilation was paused to allow brief apnea under the assigned airway-pressure condition.

Two-dimensional through-plane PC-MRI was performed using a gradient-echo sequence with retrospective ECG gating. Velocity encoding (VENC) was 150cm/s for all measurements. A single VENC of 150cm/s was selected to minimize velocity aliasing across both valve planes and body sizes and to maintain consistent acquisition settings for within-dog comparisons across recumbency and airway-pressure conditions. Imaging targets were aortic valve (AV) outflow and pulmonic valve (PV) outflow, with planes prescribed orthogonal to the ascending aorta (sinotubular junction) and proximal main pulmonary artery, respectively. Representative parameters were: field of view 300×300mm; matrix 192×256; slice thickness 6mm; repetition time/echo time 14.0/3.71ms; flip angle 15°; bandwidth 450Hz/pixel; and 25 reconstructed cardiac frames per cycle.

Flow quantification and quality control: A phase-image–based velocity overlay was used, and a region of interest (ROI) was drawn within the vessel wall and applied throughout the cardiac cycle (Fig. 1). Forward stroke volume was calculated as the integral of positive flow. Cardiac output (CO) was calculated as stroke volume × HR, and cardiac index (CI) as CO divided by body surface area, estimated as 0.101 × body weight (kg)^(2/3) (Haskins *et al.*, 2005). LV CI was derived from AV forward flow, RV CI from PV forward flow, and RV/LV CI as RV CI divided by LV CI.

Quality control included confirmation that imaging planes were prescribed perpendicular to the direction of through-plane flow, adequate luminal coverage within the vessel wall throughout the cardiac cycle, and the absence of severe velocity aliasing. Non-physiologic flow curves or frames affected by background contamination or motion/phase artifacts were excluded; acquisitions were repeated when correctable. To assess intraobserver repeatability, the same observer repeated AV and PV flow measurements after a 5-month washout interval while blinded to the first measurements. The first measurement set was used for all primary analyses, and the repeated measurement set was used only for intraobserver repeatability assessment.

Table 1: Baseline characteristics and cardiovascular screening findings of the dogs

Dog ID	Sex	Age (yr)	Body Weight (kg)	Breed	HR (bpm)	BP (mmHg) [SYS/DIA (MAP)]	Echocardiographic findings	Peak TR velocity (m/s)	Biochemical findings
A	Male	9	26	Jindo	99	101 / 66 (78)	No MR/TR	Not detected	ALT ↑217 (17–78)
B	Female	12	8.6	Beagle	99	124 / 84 (97)	Mild TR	2.10	None noted
C	Female	9	7.8	Beagle	86	96 / 55 (69)	Mild MR/TR; MMVD B1	2.70	None noted
D	Female	10	7.5	Beagle	103	110 / 70 (83)	Mild MR/TR; MMVD B1	2.86	ALP ↑465 (47–254), ALT ↑136
E	Male	16	6.8	Miniature Poodle	94	91 / 51 (64)	Mild MR/TR; MMVD B1	2.42	None noted
F	Male	10	3.5	Toy Poodle	92	91 / 51 (64)	Mild MR/TR; MMVD B1	2.89	ALP ↑398 (47–254)

Dogs with mild MR had no echocardiographic evidence of cardiac remodeling and were classified as MMVD stage B1 according to the American College of Veterinary Internal Medicine consensus guidelines (Keene *et al.*, 2019). Peak TR velocity was <3.0m/s in all dogs with measurable TR, and no dog had echocardiographic evidence of pulmonary hypertension. Abbreviations: HR, heart rate; BP, blood pressure; SYS, systolic; DIA, diastolic; MAP, mean arterial pressure; MR, mitral regurgitation; TR, tricuspid regurgitation; ALT, alanine aminotransferase; ALP, alkaline phosphatase.

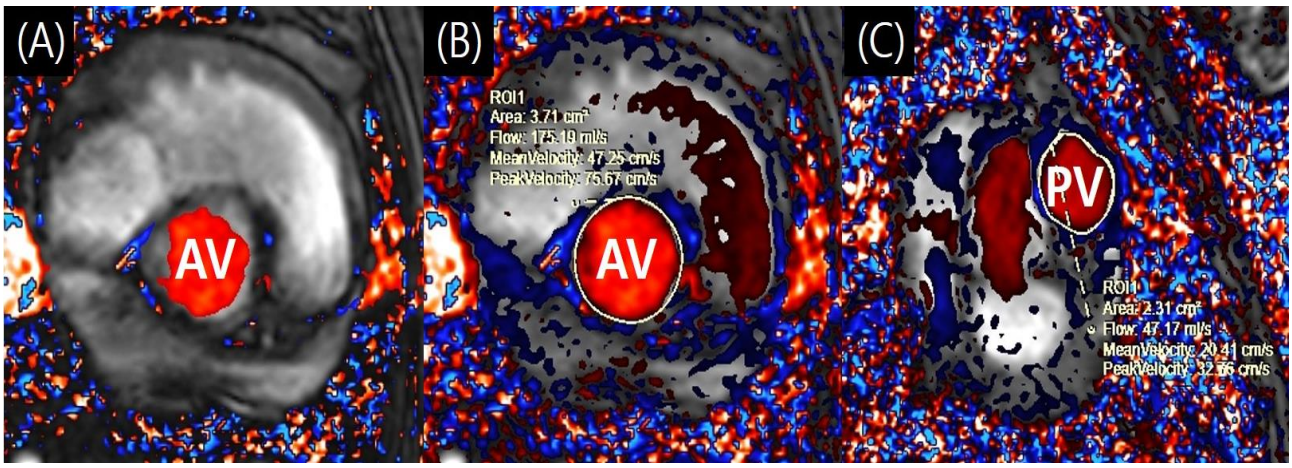

Fig. 1: Representative PC-MRI images for AV and PV flow quantification with color-scale adjustment. (A,B) Magnitude images with phase-encoded color overlays at the level of the AV acquired at the same cardiac phase. In (B), adjustment of the color scale enhances visualization of low-velocity components, allowing clearer delineation of the AV lumen and enabling precise ROI placement for quantitative through-plane flow measurement. (C) Magnitude image with phase-encoded color overlay at the level of the PV, illustrating ROI placement for pulmonary outflow assessment. Abbreviations: PC-MRI, phase-contrast magnetic resonance imaging; AV, aortic valve; PV, pulmonic valve; ROI, region of interest.

Statistical analysis: LV CI, RV CI, and RV/LV CI were analyzed as within-dog repeated measurements. Position effects under ZEEP were assessed using the Friedman test. Pairwise comparisons between positions were then performed using paired Wilcoxon signed-rank tests as exploratory post hoc analyses. Airway-pressure effects in DR were assessed using paired Wilcoxon tests (ZEEP vs CPAP 10). Because of the small sample size and exploratory nature of the paired comparisons, p-values were not adjusted for multiple comparisons and were interpreted cautiously. Mean difference, percentage change, 95% confidence interval, paired effect size (dz), and posterior probabilities were reported as complementary descriptive metrics for paired comparisons. Because of the small sample size, all inferential results, confidence intervals, and effect-size estimates were interpreted cautiously and were considered exploratory. Posterior probabilities were calculated as descriptive complementary estimates for paired comparisons. For each comparison, paired differences were defined as comparison minus baseline and modeled using a normal likelihood with a non-informative prior, $p(\mu, \sigma) \propto 1/\sigma$, for the paired mean difference and variance. The resulting posterior distribution of the paired mean difference was represented by a Student's t distribution. The posterior probability indicated the probability that the paired mean difference was in the observed direction. The posterior probability (>10%) indicated the probability that the paired mean difference exceeded 10% of the baseline mean in the observed direction; for negative mean differences, the threshold was applied in the negative direction. These probabilities were used only to describe the direction and magnitude of paired changes and were not treated as confirmatory Bayesian hypothesis tests. Intraobserver repeatability was assessed separately for LV CI derived from AV flow and RV CI derived from PV flow using 24 paired repeated observations for each measurement. Agreement between the first and repeated measurements was summarized using the intraclass correlation coefficient (ICC; two-way mixed-effects model for absolute agreement), coefficient of variation (CV%), and mean absolute difference. ICC 95% confidence intervals were estimated by bootstrap resampling.

RESULTS

Study population and acquisition stability: Flow analysis was completed in six clinically asymptomatic dogs examined in dorsal (DR), right lateral (RLR), and left lateral (LLR) recumbency (Table 1). The study population included one Jindo, three Beagles, one Miniature Poodle, and one Toy Poodle, with ages of 9–16 years and body weights of 3.5–26kg (Table 1). Mild increases in alanine aminotransferase and/or alkaline phosphatase were observed in some dogs and were recorded as non-cardiac clinical findings; their potential contribution to physiologic variability could not be fully excluded (Table 1). No dog showed evidence of pulmonary hypertension, intracardiac/extracardiac shunts, or advanced cardiac remodeling, and none received cardiovascular medication (Table 1). Heart rate and blood pressure recorded during acquisitions remained within the predefined stability ranges (Table 1).

PC-MRI quality and regurgitation screening: Representative PC-MRI images and region-of-interest placement are shown in Fig. 1. Backward flow at the aortic valve and pulmonic valve was absent or negligible (<1% of forward flow) in all dogs; regurgitation was therefore considered absent for forward-flow quantification.

Intraobserver repeatability: Intraobserver repeatability results are summarized in Table 6. Repeatability was assessed using 24 paired repeated measurements for LV CI derived from AV flow and 24 paired repeated measurements for RV CI derived from PV flow. The ICCs were 0.996 for LV CI and 0.993 for RV CI, with CVs of 2.5% and 3.0%, respectively.

Position-related changes under ZEEP: Individual dog values across recumbency positions under zero end-expiratory pressure (ZEEP) are shown in Table 2. Group summaries across recumbency positions under zero end-expiratory pressure (ZEEP) are shown in Table 3. LV cardiac index (LV CI) showed no clear overall position effect (Friedman P=0.223), whereas RV cardiac index (RV CI) showed an overall position effect (Friedman P=0.011) (Table 3). The valve-level RV/LV CI ratio remained close to unity across positions without a clear overall effect (Friedman P=0.115) (Table 3).

Table 2: Raw LV CI, RV CI, and RV/LV CI values per dog, position, and ventilatory condition

Dog ID	Position	Condition	LV CI (L/min/m²)	RV CI (L/min/m²)	RV/LV CI
A	DR	CPAP 10	2.41	1.68	0.70
A	DR	ZEEP	2.23	1.94	0.87
A	LLR	ZEEP	2.21	2.41	1.09
A	RLR	ZEEP	2.23	2.27	1.02
B	DR	CPAP 10	1.60	1.68	1.05
B	DR	ZEEP	1.86	2.00	1.08
B	LLR	ZEEP	2.03	2.25	1.11
B	RLR	ZEEP	1.93	2.13	1.10
C	DR	CPAP 10	1.70	1.58	0.93
C	DR	ZEEP	1.68	1.57	0.93
C	LLR	ZEEP	1.59	1.57	0.99
C	RLR	ZEEP	1.75	1.58	0.90
D	DR	CPAP 10	3.10	3.33	1.07
D	DR	ZEEP	3.79	3.52	0.93
D	LLR	ZEEP	4.24	4.07	0.96
D	RLR	ZEEP	4.19	3.93	0.94
E	DR	CPAP 10	2.65	2.59	0.98
E	DR	ZEEP	3.26	2.70	0.83
E	LLR	ZEEP	3.81	3.12	0.82
E	RLR	ZEEP	3.99	3.43	0.86
F	DR	CPAP 10	1.19	1.30	1.09
F	DR	ZEEP	1.25	1.33	1.06
F	LLR	ZEEP	1.35	1.51	1.12
F	RLR	ZEEP	1.38	1.61	1.17

Raw values of LV CI, RV CI, and RV/LV CI for each dog, position, and ventilatory condition (n=6 dogs). Abbreviations: LV CI, left ventricular cardiac index; RV CI, right ventricular cardiac index; RV/LV CI, ratio of PV-derived RV CI to AV-derived LV CI; DR, dorsal recumbency; RLR, right lateral recumbency; LLR, left lateral recumbency; ZEEP, zero end-expiratory pressure; CPAP 10, sustained airway pressure of 10cmH_2O during brief apnea for PC-MRI acquisition.

Table 3: LV CI, RV CI, and RV/LV CI across recumbency positions under ZEEP evaluated by Friedman test

Metric	DR (Mean±SD)	RLR (Mean±SD)	LLR (Mean±SD)	Friedman p-value
LV CI (L/min/m²)	2.35±0.98	2.58±1.20	2.54±1.20	0.223
RV CI (L/min/m²)	2.18±0.81	2.49±0.97	2.49±0.98	0.011*
RV/LV CI	0.95±0.10	1.00±0.12	1.02±0.12	0.115

Values are mean±SD. Friedman p-values refer to overall position effects under ZEEP. * indicates P<0.05.

Pairwise comparisons under ZEEP are summarized in Table 4 and Fig. 2. In exploratory unadjusted paired comparisons, RV CI was higher in both right and left lateral recumbency than in DR (P=0.031 for each comparison) (Table 4; Fig. 2). LV CI in lateral recumbency showed a directionally higher pattern than in DR (approximately 8–10%), although exploratory paired Wilcoxon tests were not significant (P=0.062 for DR vs RLR; P=0.156 for DR vs LLR) (Table 4; Fig. 2). Complementary descriptive metrics are provided in Table 4 to summarize the direction and magnitude of paired changes. No clear right–left lateral difference was observed for LV CI or RV CI (Table 4; Fig. 2). The RV/LV CI ratio showed small directional shifts; however, complementary analyses did not provide clear evidence of a meaningful recumbency-related change (Table 4; Fig. 2).

Effects of CPAP 10 in DR: Paired comparisons between ZEEP and CPAP 10 in DR are shown in Table 5 and Fig. 3. Under CPAP 10, LV CI tended to be lower than under ZEEP by approximately 10%, and RV CI tended to be lower by approximately 7% (Table 5; Fig. 3). Paired-test results did not reach P<0.05 for these comparisons; complementary descriptive metrics are provided in Table 5 to summarize the direction and magnitude of paired changes. The RV/LV CI ratio showed no appreciable change between ZEEP and CPAP 10 (Table 5; Fig. 3).

At the individual-dog level, LV CI decreased under CPAP 10 in 4/6 dogs, and RV CI decreased in 5/6 dogs (Table 2; Fig. 3).

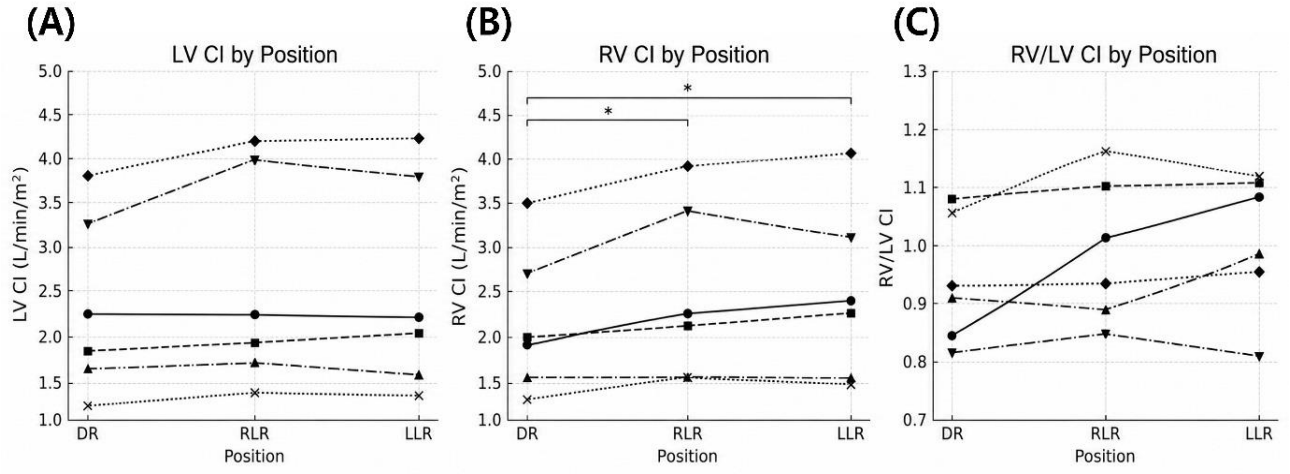

Fig. 2: Individual left ventricular cardiac index (LV CI), right ventricular cardiac index (RV CI), and RV/LV cardiac index (RV/LV CI) across recumbency positions under zero end-expiratory pressure (ZEEP). (A) LV CI, (B) RV CI, and (C) RV/LV CI are shown for dorsal recumbency (DR), right lateral recumbency (RLR), and left lateral recumbency (LLR). Each line represents an individual dog (n = 6). Distinct marker symbols and line styles were used to improve distinguishability in black-and-white reproduction. *p < 0.05 by paired Wilcoxon signed-rank test. Abbreviations: LV CI, left ventricular cardiac index; RV CI, right ventricular cardiac index; RV/LV CI, ratio of PV-derived RV CI to AV-derived LV CI; DR, dorsal recumbency; RLR, right lateral recumbency; LLR, left lateral recumbency; ZEEP, zero end-expiratory pressure.

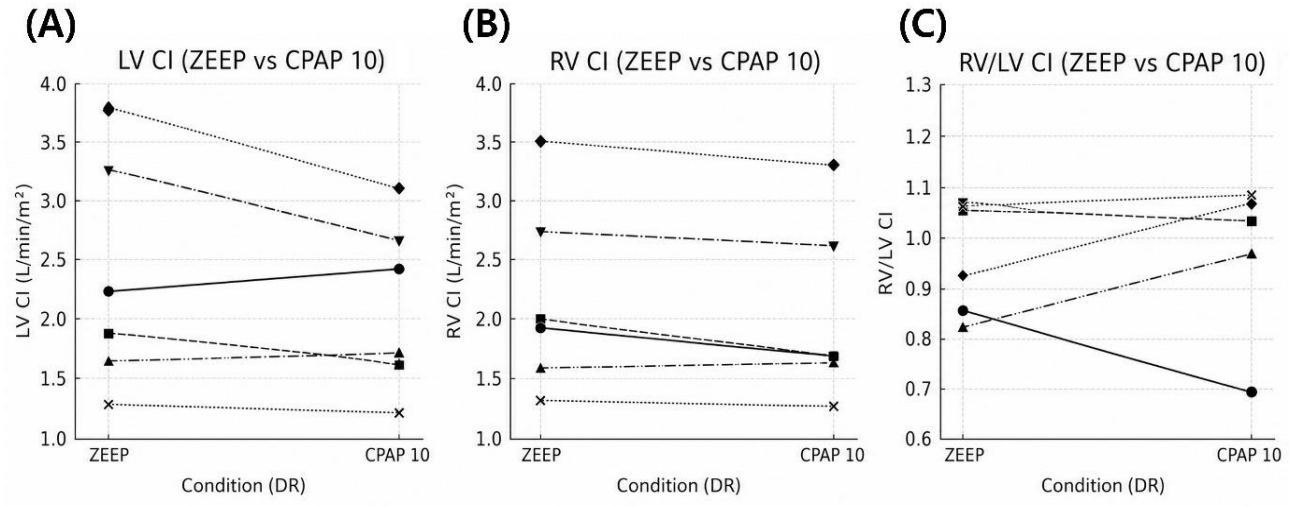

Fig. 3: Individual left ventricular cardiac index (LV CI), right ventricular cardiac index (RV CI), and RV/LV cardiac index (RV/LV CI) under zero end-expiratory pressure (ZEEP) and CPAP 10 in dorsal recumbency (DR). (A) LV CI, (B) RV CI, and (C) RV/LV CI are shown for each dog (n = 6). Each line represents an individual dog. Distinct marker symbols and line styles were used to improve distinguishability in black-and-white reproduction. Abbreviations: LV CI, left ventricular cardiac index; RV CI, right ventricular cardiac index; RV/LV CI, ratio of PV-derived RV CI to AV-derived LV CI; DR, dorsal recumbency; ZEEP, zero end-expiratory pressure; CPAP 10, sustained airway pressure of 10cmH_2O during brief apnea for PC-MRI acquisition.

Table 4: Pairwise comparisons of LV CI, RV CI, and RV/LV CI between positions under ZEEP

Metric	Comparison	Mean diff	Δ%	CI_95	Wilcoxon p-value	dz	Posterior probability	Posterior probability (>10%)
LV CI	DR vs RLR	0.232	9.902	-0.06 to 0.53	0.062	0.833	0.952	0.492
LV CI	DR vs LLR	0.189	8.043	-0.08 to 0.46	0.156	0.732	0.934	0.340
LV CI	RLR vs LLR	-0.044	-1.692	-0.16 to 0.07	0.562	-0.394	0.811	0.003
RV CI	DR vs RLR	0.318	14.598	0.05 to 0.58	0.031*	1.264	0.987	0.813
RV CI	DR vs LLR	0.315	14.503	0.10 to 0.53	0.031*	1.541	0.994	0.853
RV CI	RLR vs LLR	-0.002	-0.083	-0.19 to 0.18	0.844	-0.012	0.511	0.009
RV/LV CI	DR vs RLR	0.049	5.157	-0.02 to 0.12	0.219	0.735	0.934	0.076
RV/LV CI	DR vs LLR	0.067	7.114	-0.02 to 0.15	0.062	0.843	0.953	0.220
RV/LV CI	RLR vs LLR	0.019	1.862	-0.04 to 0.08	0.562	0.323	0.768	0.009

Mean diff and Δ% are expressed as the second-listed condition minus the first-listed condition for each comparison. CI_95 denotes the 95% confidence interval for the mean difference. Wilcoxon p-values are from exploratory unadjusted paired comparisons; *p < 0.05. Because no adjustment for multiple comparisons was applied, p-values should be interpreted cautiously. dz indicates paired effect size. Posterior probability indicates the probability that the paired mean difference was in the observed direction. Posterior probability (>10%) indicates the probability that the paired mean difference exceeded 10% of the baseline mean in the observed direction. These probabilities are descriptive complementary estimates and were not used as confirmatory hypothesis tests. Abbreviations: LV CI, left ventricular cardiac index; RV CI, right ventricular cardiac index; RV/LV CI, ratio of PV-derived RV CI to AV-derived LV CI; DR, dorsal recumbency; RLR, right lateral recumbency; LLR, left lateral recumbency; ZEEP, zero end-expiratory pressure.

Table 5: Paired comparisons of LV CI, RV CI, and RV/LV CI between ZEEP and CPAP 10 in dorsal recumbency

Metric	DR-ZEEP (mean±SD)	DR-CPAP 10 (mean±SD)	Mean diff	Δ%	CI_95	Wilcoxon p-value	dz	Posterior probability	Posterior probability (>10%)
LV CI	2.35±0.98	2.11±0.73	-0.239	-10.169	-0.61 to 0.13	0.219	-0.683	0.922	0.511
RV CI	2.18±0.81	2.03±0.77	-0.148	-6.820	-0.28 to -0.01	0.062	-1.148	0.981	0.123
RV/LV CI	0.95±0.10	0.97±0.15	0.021	2.222	-0.10 to 0.15	0.844	0.177	0.658	0.095

DR-ZEEP and DR-CPAP 10 values are mean±SD. Mean diff and Δ% are expressed as CPAP 10 − ZEEP. CI_95 denotes the 95% confidence interval for the mean difference. Wilcoxon p-values are from exploratory unadjusted paired comparisons; *P<0.05. Because no adjustment for multiple comparisons was applied, p-values should be interpreted cautiously. Posterior probability indicates the probability that the paired mean difference was in the observed direction. Posterior probability (>10%) indicates the probability that the paired mean difference exceeded 10% of the baseline mean in the observed direction. These probabilities are descriptive complementary estimates and were not used as confirmatory hypothesis tests. Abbreviations: LV CI, left ventricular cardiac index; RV CI, right ventricular cardiac index; RV/LV CI, ratio of PV-derived RV CI to AV-derived LV CI; DR, dorsal recumbency; RLR, right lateral recumbency; LLR, left lateral recumbency; ZEEP, zero end-expiratory pressure; CPAP 10, sustained airway pressure of 10cmH_2O during brief apnea for PC-MRI acquisition.

Table 6: Intraobserver repeatability of PC-MRI flow measurements

Measurement	Paired observations	ICC (95% CI)	CV (%)	Mean absolute difference (L/min/m²)
LV CI from AV flow	24	0.996 (0.991–0.999)	2.5	0.06
RV CI from PV flow	24	0.993 (0.985–0.997)	3.0	0.08

Intraobserver repeatability was assessed by repeated measurements performed by the same observer after a 5-month washout interval. The first measurement set was used for the primary analyses, and the repeated measurement set was used only for repeatability assessment. ICC was calculated using a two-way mixed-effects model for absolute agreement. CV was calculated from the standard deviation of paired differences divided by √2 and expressed relative to the grand mean of the first and repeated measurements. ICC 95% CIs were estimated by bootstrap resampling. Abbreviations: PC-MRI, phase-contrast magnetic resonance imaging; ICC, intraclass correlation coefficient; CI, confidence interval; CV, coefficient of variation; LV CI, left ventricular cardiac index; RV CI, right ventricular cardiac index; AV, aortic valve; PV, pulmonic valve.

DISCUSSION

This study examined within-dog variation in 3.0T PC-MRI–derived ventricular cardiac indices across recumbency and airway-pressure conditions in anesthetized dogs. Under ZEEP, LV CI tended to be modestly higher in lateral recumbency than in DR, but this directional pattern was less consistent across dogs than that observed for RV CI. In contrast, RV CI showed a clearer positional pattern, with lateral recumbency associated with larger mean increases than those seen for LV CI. Across conditions, the valve-level RV/LV CI ratio remained within a narrow range, suggesting no large apparent imbalance between PV-derived and AV-derived forward-flow indices under the tested conditions. In DR, LV CI and RV CI showed non-significant directional decreases under CPAP 10, while RV/LV CI showed minimal change. These findings should be interpreted within the technical and physiologic context of veterinary CMR, in which PC-MRI flow quantification can be influenced by plane prescription, VENC selection, background phase effects, and ROI placement, while canine CMR examinations are commonly performed under general anesthesia and controlled ventilation (Gatehouse *et al.*, 2005; Nayak *et al.*, 2015; Drees *et al.*, 2015; Fries, 2024). Therefore, recumbency and airway-pressure conditions should be considered part of the physiologic acquisition environment rather than merely technical settings during canine PC-MRI. Similarly, the standardized butorphanol–propofol–isoflurane protocol with controlled mechanical ventilation was selected to support reproducible ECG-gated acquisition and continuous physiologic monitoring, but it should be regarded as part of the physiologic acquisition environment rather than a hemodynamically neutral background condition (Hopper and Powell, 2013; Drees *et al.*, 2015; Bailey *et al.*, 2025).

Recumbency is not a neutral background condition during canine anesthesia (Bornscheuer *et al.*, 1996). Prior experimental work in anesthetized dogs has described position-dependent cardiopulmonary changes, including differences in arterial pressure, systemic vascular resistance, and indices of cardiac work, with DR often linked to less favorable global performance than lateral positions (Bornscheuer *et al.*, 1996). Under controlled ventilation, gravitational shifts in lung aeration and abdominal organ position may also alter venous return and pulmonary vascular loading (Bornscheuer *et al.*, 1996; Ambrisko *et al.*, 2017). Within this physiologic framework, the higher RV CI observed during lateral recumbency compared with DR is compatible with

recumbency-related differences in right-sided loading conditions under controlled mechanical ventilation, although time-dependent anesthetic effects cannot be fully excluded because the acquisition order was fixed (Bornscheuer *et al.*, 1996; Ambrisko *et al.*, 2017).

The more prominent positional pattern for RV CI than for LV CI is also consistent with established ventricular physiology. The RV is sensitive to changes in pulmonary vascular load and venous return, and moderate shifts in intrathoracic conditions may translate into measurable changes in RV output (Naeije and Badagliacca, 2017). In the present study, LV CI showed smaller and less consistent positional changes than RV CI despite physiologic control of HR and MAP. This may reflect relatively greater buffering of LV output to modest loading variation under these conditions. For LV CI, complementary descriptive estimates summarized the direction and magnitude of paired differences; however, these estimates were interpreted cautiously because the paired LV CI tests were not statistically significant and the sample size was small. Taken together, these findings suggest that RV-derived indices may be more sensitive to recumbency-related shifts under anesthesia, while LV-derived indices may show smaller and less uniform responses.

Notably, differences between RLR and LLR were small for LV CI, RV CI, and RV/LV CI. This pattern aligns with findings that, under controlled conditions, ventilation distribution in right and left lateral recumbency is broadly similar at a global level, despite potential side-dependent regional variation (Ambrisko *et al.*, 2017). In practical terms, the main observed contrast in this dataset was DR versus lateral recumbency, rather than right versus left lateral recumbency; however, this pattern should be interpreted cautiously because the position sequence was not randomized.

In DR, LV CI and RV CI tended to be lower under CPAP 10 than under ZEEP, but these paired comparisons did not reach statistical significance. Positive airway pressure raises intrathoracic pressure and can reduce venous return and ventricular filling, thereby lowering stroke volume and cardiac output in susceptible settings; this mechanism is relevant to anesthetized and mechanically ventilated dogs because airway pressure can alter pulmonary mechanics and cardiopulmonary loading during image acquisition (Soares *et al.*, 2021; Rodrigues *et al.*, 2022; Mosing *et al.*, 2025). These mechanisms differ from those of recumbency, which are more likely to influence cardiopulmonary loading through gravitational effects on lung aeration and abdominal organ position (Bornscheuer *et al.*, 1996; Ambrisko *et al.*, 2017). These mechanisms provide a physiologic basis for the directional changes observed in PC-MRI–derived indices despite stable routine monitoring.

The absence of a consistent shift in RV/LV CI under CPAP 10 suggests that PV-derived and AV-derived forward-flow indices changed proportionally in this dataset, but this should not be interpreted as definitive evidence that airway pressure affected both ventricles equally. This pattern is compatible with prior canine and human PC-MRI observations in which common peri-anesthetic or measurement-related changes may alter absolute flow values while preserving proportional relationships between the pulmonary and systemic circulations (Gatehouse *et al.*, 2005; Drees *et al.*, 2015; Nayak *et al.*, 2015). In clinical and research settings, this suggests that airway-pressure conditions may contribute to small directional changes in LV CI and RV CI. Therefore, airway-pressure conditions should be documented and standardized when comparing serial or group-level PC-MRI flow measurements in dogs.

Clinical implications: These findings have practical implications for small-animal cardiac MRI performed under anesthesia. First, the observed 7–15% directional changes in ventricular cardiac indices should not be interpreted as validated clinically meaningful thresholds for individual dogs. Rather, their main relevance is methodological: differences of this magnitude could confound comparisons across time points or between study groups if recumbency and airway-pressure conditions are not standardized, even when heart rate and arterial pressure are maintained within predefined limits (Bornscheuer *et al.*, 1996, Drees *et al.*, 2015). This supports treating positioning and ventilatory strategy as part of the hemodynamic environment of the scan and as standardization variables, rather than as purely technical acquisition choices. Standardizing recumbency and airway-pressure settings may therefore improve comparability of flow-based metrics in future work. Further studies are needed to determine whether changes of this magnitude have direct clinical consequences in dogs with cardiac or pulmonary disease.

Second, RV/LV CI remained relatively stable across the tested conditions. In this small cohort of clinically asymptomatic dogs without pulmonary hypertension, intracardiac/extracardiac shunts, or advanced cardiac remodeling, the relative stability of RV/LV CI suggests that no large imbalance was detected between PV-derived and AV-derived forward-flow indices under the tested conditions. However, similar proportional stability should not be assumed in dogs with conditions that uncouple pulmonary and systemic forward flow (e.g., clinically important left-to-right shunts such as patent ductus arteriosus or septal defects, or substantial valvular regurgitation such as advanced MMVD with marked MR), or in dogs with pulmonary hypertension and other right-sided pressure/volume overload in which RV function and stroke volume may be disproportionately affected (Fratz *et al.*, 2013; Nayak *et al.*, 2015; Sargent *et al.*, 2015; Feldhütter *et al.*, 2022; Yuchi *et al.*, 2023). In such patients, a comparable absolute change in LV CI or RV CI could be more clinically consequential, and shifts in RV/LV CI might carry different implications. Therefore, RV/LV CI should be interpreted as a valve-level forward-flow ratio rather than a direct measure of intrinsic biventricular output balance.

Overall, the findings should be interpreted as preliminary exploratory estimates rather than normal reference values or definitive benchmarks.

Limitations: Several limitations should be considered. First, the sample size was small (n=6), and the dogs were heterogeneous in age, breed, body size, sex, and mild valvular findings. Because of the small cohort, sex-related effects on PC-MRI–derived LV CI, RV CI, and RV/LV

CI could not be evaluated separately. No formal a priori power calculation was performed because reliable effect-size estimates for recumbency- and airway-pressure-related changes in canine 3.0T PC-MRI flow indices were not available. Therefore, the study was underpowered for detecting modest hemodynamic differences, and the reported confidence intervals, effect sizes, and posterior probabilities should be interpreted as exploratory and potentially unstable estimates. Because the exploratory paired comparisons were not adjusted for multiple testing, statistically significant paired-test findings should also be interpreted cautiously, and type I error cannot be excluded. Because regurgitation can influence the relationship between forward flow and ventricular output, it remains a potential source of variability; however, the regurgitation in this study was mild and without remodeling, making large regurgitant-load shifts from recumbency or airway-pressure changes less likely (Sargent *et al.*, 2015). Accordingly, RV/LV CI should be interpreted as the ratio of PV-derived to AV-derived valve-level forward-flow indices, because mild MR/TR, AV/PV plane prescription, and respiratory loading may influence this ratio despite the absence of clinically important regurgitation or pulmonary hypertension (Gatehouse *et al.*, 2005, Nayak *et al.*, 2015, Sargent *et al.*, 2015). Stratified analyses by body size or regurgitation status were not feasible, and the results should be interpreted as preliminary estimates of effect patterns and magnitudes rather than definitive reference values. In addition, all measurements were performed using 2D PC-MRI with fixed planes and a single VENC setting. Two-dimensional acquisition cannot capture in-plane velocity components, and a single VENC of 150cm/s may be suboptimal across valves, body sizes, and flow states. Although this setting was selected to reduce the risk of velocity aliasing and to maintain consistent acquisition conditions, it may have reduced sensitivity to lower-velocity components and may not have been optimal for all individual valve planes (Gatehouse *et al.*, 2005, Nayak *et al.*, 2015). Systematic quality control was applied, but small degrees of under- or overestimation cannot be fully excluded (Westenberg *et al.*, 2008; Dyverfeldt *et al.*, 2015). Although intraobserver repeatability was assessed and showed high agreement, interobserver variability was not evaluated. Small differences in AV plane prescription relative to the sinotubular junction may also influence flow estimates, and future studies should further standardize AV plane placement in the proximal ascending aorta.

Physiologic variability intrinsic to prolonged anesthesia is another important limitation. Although a standardized butorphanol–propofol–isoflurane protocol with controlled mechanical ventilation was used in all dogs, anesthetic drugs and mechanical ventilation may directly or indirectly affect cardiovascular and respiratory variables; therefore, protocol-related effects cannot be fully excluded (Hopper and Powell, 2013; Drees *et al.*, 2015; Bailey *et al.*, 2025). Although HR and arterial pressure were monitored and data were acquired only during predefined stable periods, the acquisition order was fixed rather than randomized or counterbalanced. Therefore, position-related differences may have been confounded by time under anesthesia, cumulative anesthetic exposure, fluid administration, body temperature changes, physiologic drift, or repeated brief apnea (Bailey *et al.*, 2025). Time-dependent effects could not be fully separated from posture- or airway-pressure-related effects in this study. Future studies should use larger randomized or counterbalanced crossover designs to distinguish recumbency effects from time-dependent anesthetic and ventilatory influences.

Conclusions: In anesthetized dogs examined at 3.0T, PC-MRI–derived ventricular cardiac indices showed modest, directional within-dog variation across recumbency and airway-pressure conditions, although the small and heterogeneous cohort limits generalization. These preliminary findings are mainly relevant for research standardization and support standardized documentation of acquisition conditions, but their direct clinical significance and generalizability require confirmation in larger randomized or counterbalanced studies.

Funding: No funding was received for this study.

Acknowledgment: The authors thank the dog owners for their participation and cooperation.

Conflict of Interest: The authors declare that the research was conducted in the absence of any commercial or financial relationships that could be construed as a potential conflict of interest.

Data Availability: All data generated or analyzed during this study are included in this published article. Additional information is available from the corresponding author upon reasonable request.

Ethics Statement: The animal study protocol was reviewed and approved by the Institutional Animal Care and Use Committee of Jeonbuk National University (approval No. JBNU NON2025-059).

Authors Contribution: CL and HY conceived and designed the study. CL and HY acquired the data. CL, KL and HY analyzed and interpreted the data. CL drafted the manuscript. All authors critically revised the manuscript and approved the final version.

Generative AI Statement: A generative AI tool was used only for language polishing, grammar and typographical checks, terminology consistency, and formatting review after the manuscript had been drafted by the authors. The authors reviewed and edited all AI-assisted suggestions and take full responsibility for the final content of the manuscript.

REFERENCES

Adriaans BP, Westenberg JJM, van Cauteren YJM, *et al.*, 2020. Clinical assessment of aortic valve stenosis: Comparison between 4D flow MRI and transthoracic echocardiography. Journal of Magnetic Resonance Imaging 51:472-480.

Ambrisko TD, Schramel JP, Auer U, *et al.*, 2017. Impact of four different recumbencies on the distribution of ventilation in conscious or

anaesthetized spontaneously breathing beagle dogs: An electrical impedance tomography study. PLOS ONE 12:e0183340.

Ambrósio AM, Sanchez AF, Pereira MAA, *et al.*, 2022. Assessment of Regional Ventilation During Recruitment Maneuver by Electrical Impedance Tomography in Dogs. Frontiers in Veterinary Science 8:815048.

Bailey K, Briley J, Duffee L, *et al.*, 2025. The American College of Veterinary Anesthesia and Analgesia Small Animal Anesthesia and Sedation Monitoring Guidelines 2025. Veterinary Anaesthesia and Analgesia 52:377-385.

Bornscheuer A, Mahr KH, Bötel C, *et al.*, 1996. Cardiopulmonary effects of lying position in anesthetized and mechanically ventilated dogs. Journal of Experimental Animal Science 38:20-27.

Drees R, Johnson RA, Stepien RL, *et al.*, 2015. Effects of two different anesthetic protocols on cardiac flow measured by two dimensional phase contrast magnetic resonance imaging. Veterinary Radiology & Ultrasound 56:168-175.

Dyverfeldt P, Bissell M, Barker AJ, *et al.*, 2015. 4D flow cardiovascular magnetic resonance consensus statement. Journal of Cardiovascular Magnetic Resonance 17:72.

Feldhütter EK, Domenech O, Vezzosi T, *et al.*, 2022. Right ventricular size and function evaluated by various echocardiographic indices in dogs with pulmonary hypertension. Journal of Veterinary Internal Medicine 36:1882-1891.

Fratz S, Chung T, Greil GF, *et al.*, 2013. Guidelines and protocols for cardiovascular magnetic resonance in children and adults with congenital heart disease: SCMR expert consensus group on congenital heart disease. Journal of Cardiovascular Magnetic Resonance 15:51.

Fries RC, 2024. Current use of cardiac MRI in animals. Journal of Veterinary Cardiology 51:13-23.

Gärtner K, Bornscheuer A, Kunstyr I, *et al.*, 1996. [Dorsal recumbency in dogs--a circulatory risk during surgical treatment?]. Tierärztliche Praxis 24:596-599.

García-Sanz V, Canfrán S, Gómez de Segura IA, *et al.*, 2020. Effect of recumbency and body condition score on open-lung positive end-expiratory pressure and respiratory system compliance following a stepwise lung recruitment manoeuvre in healthy dogs during general anaesthesia. Research in Veterinary Science 132:177-185.

Gatehouse PD, Keegan J, Crowe LA, *et al.*, 2005. Applications of phase-contrast flow and velocity imaging in cardiovascular MRI. European Radiology 15:2172-2184.

Gilbert SH, McConnell FJ, Holden AV, *et al.*, 2010. The potential role of MRI in veterinary clinical cardiology. The Veterinary Journal 183:124-134.

Haskins S, Pascoe PJ, Ilkiw JE, *et al.*, 2005. Reference cardiopulmonary values in normal dogs. Comparative Medicine 55:156-161.

Hillis GS and Bloomfield P, 2005. Basic transthoracic echocardiography. BMJ 330:1432-1436.

Hopper K and Powell LL, 2013. Basics of mechanical ventilation for dogs and cats. Veterinary Clinics of North America: Small Animal Practice 43:955-969.

Keene BW, Atkins CE, Bonagura JD, *et al.*, 2019. ACVIM consensus guidelines for the diagnosis and treatment of myxomatous mitral valve disease in dogs. Journal of Veterinary Internal Medicine 33:1127-1140.

Kramer CM, Barkhausen J, Bucciarelli-Ducci C, *et al.*, 2020. Standardized cardiovascular magnetic resonance imaging (CMR) protocols: 2020 update. Journal of Cardiovascular Magnetic Resonance 22:17.

Mosing M, Waldmann AD, Gent TC, *et al.*, 2025. Impact of positive end-expiratory pressure and recruitment maneuver on healthy lungs in dogs assessed by functional and anatomical monitoring methods. Frontiers in Veterinary Science 12:1545683.

Naeije R and Badagliacca R, 2017. The overloaded right heart and ventricular interdependence. Cardiovascular Research 113:1474-1485.

Nayak KS, Nielsen JF, Bernstein MA, *et al.*, 2015. Cardiovascular magnetic resonance phase contrast imaging. Journal of Cardiovascular Magnetic Resonance 17:71.

Riquelme M, Monnet E, Kudnig ST, *et al.*, 2005. Cardiopulmonary effects of positive end-expiratory pressure during one-lung ventilation in anesthetized dogs with a closed thoracic cavity. American Journal of Veterinary Research 66:978-983.

Rodrigues RR, Ambrósio AM, Engbruch AM, *et al.*, 2022. Intraoperative protective mechanical ventilation in dogs: A randomized clinical trial. Frontiers in Veterinary Science 9:842613.

Sanchez AF, Ambrósio AM, Pinto A, *et al.*, 2024. Effects of a stepwise alveolar recruitment maneuver on lung volume distribution in dogs assessed by computed tomography. Frontiers in Veterinary Science 10:1232635.

Sargent J, Connolly DJ, Watts V, *et al.*, 2015. Assessment of mitral regurgitation in dogs: comparison of results of echocardiography with magnetic resonance imaging. Journal of Small Animal Practice 56:641-650.

Soares JHN, Braun C, Machado ML, *et al.*, 2021. Cardiovascular function, pulmonary gas exchange and tissue oxygenation in isoflurane-anesthetized, mechanically ventilated Beagle dogs with four levels of positive end-expiratory pressure. Veterinary Anaesthesia and Analgesia 48:324-333.

Westenberg JJ, Roes SD, Ajmone Marsan N, *et al.*, 2008. Mitral valve and tricuspid valve blood flow: accurate quantification with 3D velocity-encoded MR imaging with retrospective valve tracking. Radiology 249:792-800.

Yuchi Y, Suzuki R, Saito T, *et al.*, 2023. Echocardiographic characteristics of dogs with pulmonary hypertension secondary to respiratory diseases. Journal of Veterinary Internal Medicine 37:1656-1666.